Earth-Based Radar Observations of Venus
Multi-Look Map Products

July 2021
Bruce A. Campbell
Smithsonian Institution

1.0 Summary

This archive contains maps of radar backscatter from Venus assembled from individual looks collected in observing runs from 1988 to 2020. Those looks are also archived in delay-Doppler format with the PDS, and the documentation for that archive details the data collection steps (https://pds-geosciences.wustl.edu/missions/venus_radar/index.htm). [Campbell, 2016]. In all but the 2012 dataset, the echoes were transmitted from and received at the Arecibo Observatory. In 2012 the Green Bank Telescope was used as a receiver (Table 1). For each observing year with Venus close to inferior conjunction, there are multi-look views of the "northern" and "southern" hemispheres, defined with respect to the sub-radar point latitude and longitude during the period. All maps are referenced to a 335 E projection longitude. Each map set contains an image in the opposite-sense circular polarization (OCP, sometimes called "polarized") and one in the same-sense circular polarization (SCP, sometimes called "depolarized"). Spatial sampling is at 1 km per pixel, or about 106 pixels per degree on Venus. The individual looks are normalized to the background noise level such that the OCP and SCP mosaics can be ratioed to obtain the circular polarization ratio (CPR). Offsets of order ten pixels with respect to the Magellan-defined cartographic grid may exist across the images and between observing years.

Table 1. Observing and Mapping Parameters

Frequency	2380 MHz
Wavelength	12.6 cm
Baud	3.8 μs – 4.0 μs
Signal Coding	8191-length pseudo-random noise (PN)
Bandwidth	263 kHz – 250 kHz
Transmitter	Arecibo Observatory
Receiver	Arecibo (1988, 2015, 2017, 2020) Green Bank Telescope (2012)
Polarization	Same-sense circular (SCP) Opposite-sense circular (OCP)
Map Projection	Sinusoidal equal-area
Map resolution	1 km per pixel for 6051.0 km radius
Map size	20,000 columns x 12,000 rows
Map Center Longitude	335^{o} E

2.0 Data Processing

Mapping of a single 5-minute radar look to a latitude-longitude framework requires a matrix transformation based on knowledge of the sub-radar point (SRP) location, the limb-to-limb bandwidth due to the rotation rate of the Earth and Venus, and the "Doppler angle" between the north-south axis of the planet and the apparent axis of rotation. These values may come from ephemerides or from fitting to the delay-Doppler locations of points of known latitude and longitude. In practice, there are small uncertainties in each value, leading to low-order distortions in the locations of features across such large areas of the disk.

The mosaicking process warps the OCP looks of any given observing year to tie-points in the first look of that period. Up to 60 tiepoints are chosen manually for widely distributed sites with high backscatter and sharp features. This leads to reasonable fitting of surfaces features at about the 1-2 km limit of the raw data (Fig. 1). The SCP looks are then warped using the same coefficients, so the two images have identical geometry and can be used to form the CPR after additional averaging to reduce speckle effects. The quality of the 2012 maps is about a factor of two worse in spatial resolution than other years due to unresolved phase stability issues from the receiver setup. The maps are 20,000 columns by 12,000 rows, with the lower edge of the northern hemisphere maps at 25 S and the upper edge of the southern hemisphere maps at 20 N. The map projection is sinusoidal equal-area, with a scale of 105.6099 pixels per degree (1-km horizontal sampling for a 6051.0 km planetary radius).

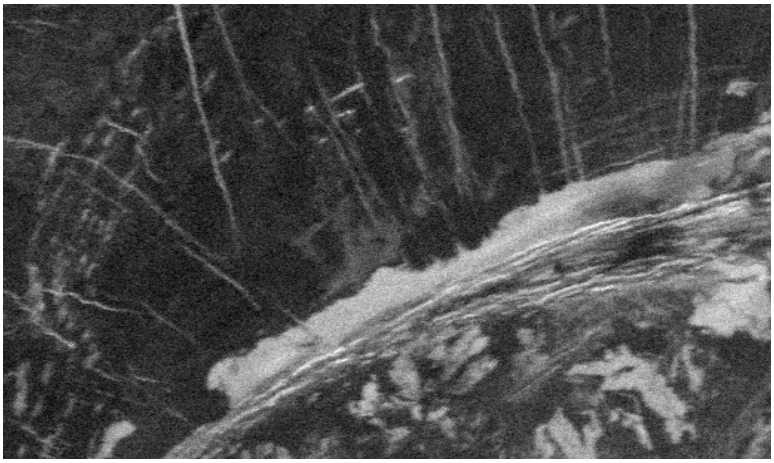

Fig. 1. Opposite-sense circular (OCP) image of northern Lada Terra on Venus from 2017 Arecibo observations. About 30 looks have been co-registered and summed. Detail of fine fractures and lineaments are preserved by accurate registration.

The mosaicked images are truncated to an incidence angle range of 76º in order to avoid the fold-over of the very bright sub-radar region into delays greater than the time window of each pulse (8191 samples at the baud for that year in Table 2). Coverage of each hemisphere differs with the latitude of the SRP (Table 2), which cycles through values of about +8º (2015), ±3º (1988, 2012, 2020) and about -9º (2017). More southerly SRP locations reveal a greater area toward the south pole (e.g., Lada Terra), while northern excursions of the SRP show features at higher

northern latitude (e.g., Maxwell Montes) (Fig. 2). The regions near the sub-radar point are truncated to incidence angles >15º, as the spatial resolution in the range direction exceeds 3 km at this angle. As an arbitrary limit, the maps are also cut off within 450 km of the Doppler equator where folding from the opposite hemisphere is extreme.

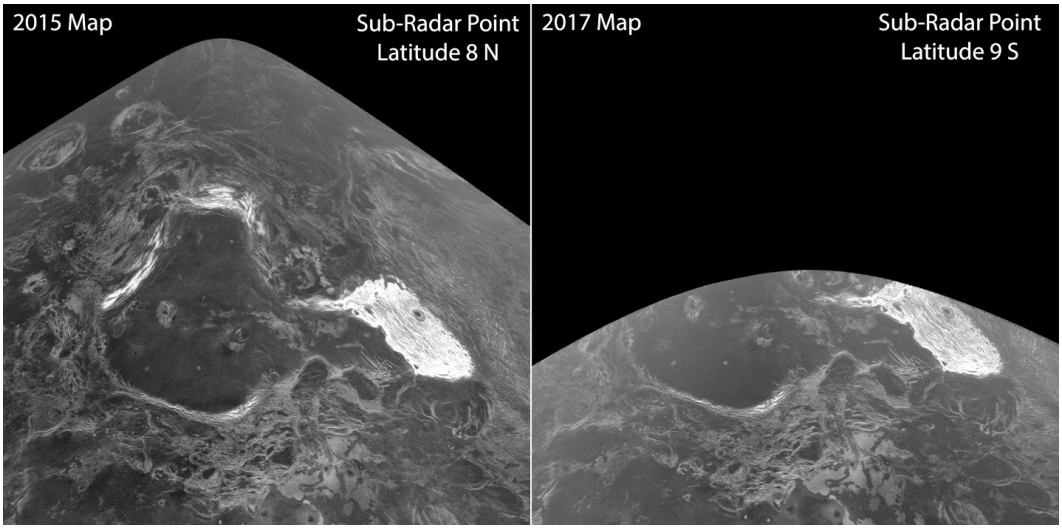

Fig. 2. Comparison of coverage area on Venus with varying sub-radar point latitude. Maximum span of sub-radar point latitude at conjunction is between about 8 N and 9 S. When the SRP is in the northern hemisphere (left) much more of the higher northern latitudes are visible. Both images are truncated at 76º incidence angle.

3.0 Georeferencing and North-South Ambiguity

In using the multi-look mosaics for geologic mapping or change detection, care must be used in identifying features that are folded over from one hemisphere to the other by their identical position in delay and Doppler space. In any single look these folded features are sharp and often readily apparent, such as Maxwell Montes appearing in the southern hemisphere or Alpha Regio appearing in the north. The summing of many looks representing several days of observations will smear these echoes and reduce their brightness relative to fixed features that are in the actual mapped hemisphere (Fig. 3). These echoes never fully disappear, and bright lineaments, craters, or a general "haze" may still be evident, especially on radar-dark terrain of the desired hemisphere. With a number of maps from different observing years, coverage of areas without N-S folded features in one year may be substituted for poorer data in other maps. This is especially effective for the SCP maps, which have less sensitivity to incidence angles changes.

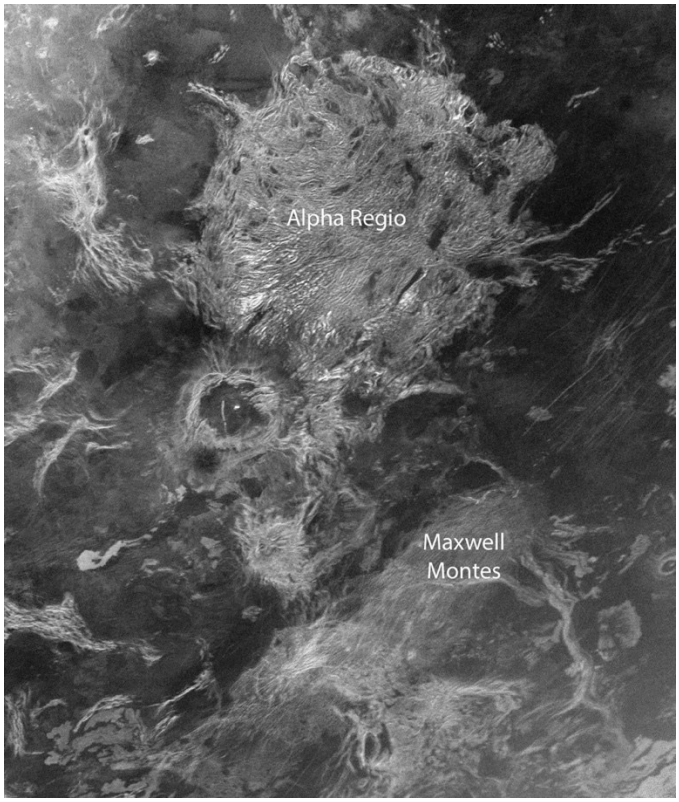

Fig. 3. Radar image from 2015 of Alpha Regio. The oval bright feature south of Alpha is the folded-over image of Maxwell Montes in the northern hemisphere. Multi-look summing blurs and reduces the echo strength of such N-S folded features, but they can clearly impact geologic studies.

4.0 Power Calibration and Browse Images

Each 32-bit radar look is normalized to the background noise, and the mosaicked maps are averaged in power by the number of summed looks. In principle, these "SNR" values would be comparable among all observing years, but there are changes over time in the transmitted power and in the gain of the antenna(s). In particular, the 1988 data were collected prior to the upgrade of the S-band transmitter, so the power level is several dB below that in 2015 and 2017. The 2012 data were collected using Green Bank for reception, with a loss of gain due to the smaller antenna. Finally, the 2020 data were collected with only one-half of the possible transmit power, and with the dish gain down about 2 dB due to hurricane damage. Absolute calibration of the data to values of the dimensionless "sigma-zero" backscatter coefficient is only achievable by comparison to swaths of the Magellan data with similar incidence angle [Campbell et al., 1999].

We can derive an offset value to bring the maps into approximate calibration in echo power. Because the region near the sub-radar point in every observation is on regional plains, the scattering behavior with incidence angle, ϕ, is expected to be relatively similar. Plots of a third-order polynomial fit to the mean echo power for each year against incidence angle do show similar trends, with offsets related to the effects of transmitter power and antenna-related gains (Fig. 4). Based on these offsets, calibration factors relative to the 2017 observations (for 20^o-30^o incidence angle) are presented in Table 2. By adding these factors to both polarizations, the CPR values will

remain consistent over all datasets. The effects of the transmitter upgrade are apparent between 1988 and later years, with that advantage partly lost in using the GBT for 2012. The 2020 data are, as expected, also significantly lower in power than the 2017 runs and barely comparable to 1988 for the northern hemisphere.

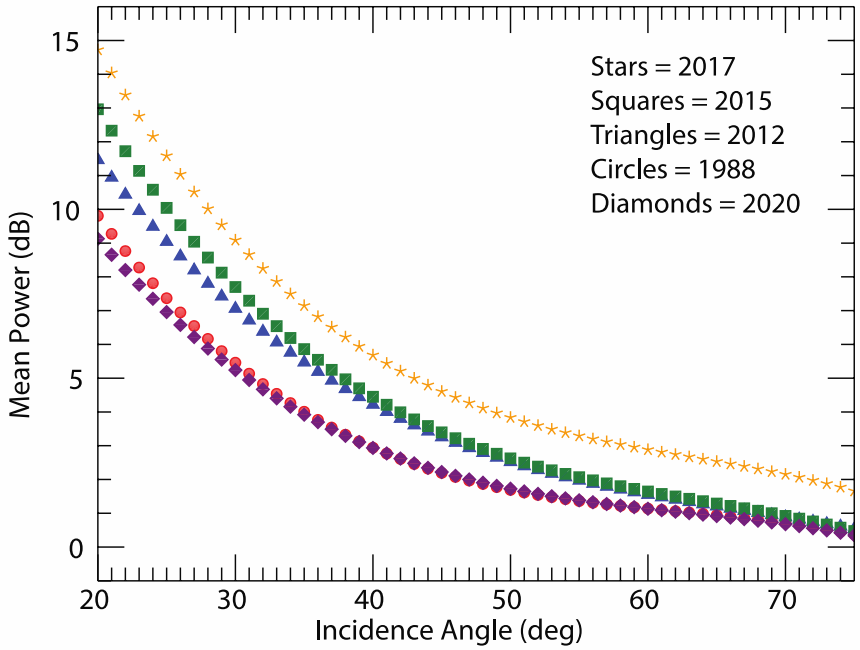

Fig. 4. Plot of mean echo power (dB), relative to the noise background, versus incidence angle for northern-hemisphere observations from 1988, 2012, 2015, 2017, and 2020.

The northern-hemisphere OCP scattering function for 2017, which can be used to normalize image maps for easier comparison, is given by:

$$P_{dB}(\phi) = 35.34 - 1.41\phi + 0.021\phi^2 - 0.00011\phi^3$$

where the values of ϕ are in degrees. The archive contains a 32-bit map of the incidence angle across the entire visible disk for each hemisphere, though the cutoffs at 15° and 76° will truncate actual image coverage. A TIFF browse version of each map, normalized to the 2017 scatter law for OCP, is provided for easy reference (Fig. 5). The SCP browse maps are normalized to cos(ϕ), consistent with scattering functions for other planetary surfaces (Fig. 6). The 32-bit data files are in linear-format power scaled to the noise background, while the TIFF images represent an ad-hoc log-scale (dB) with 8-bit range chosen to capture most of the image detail without saturation.

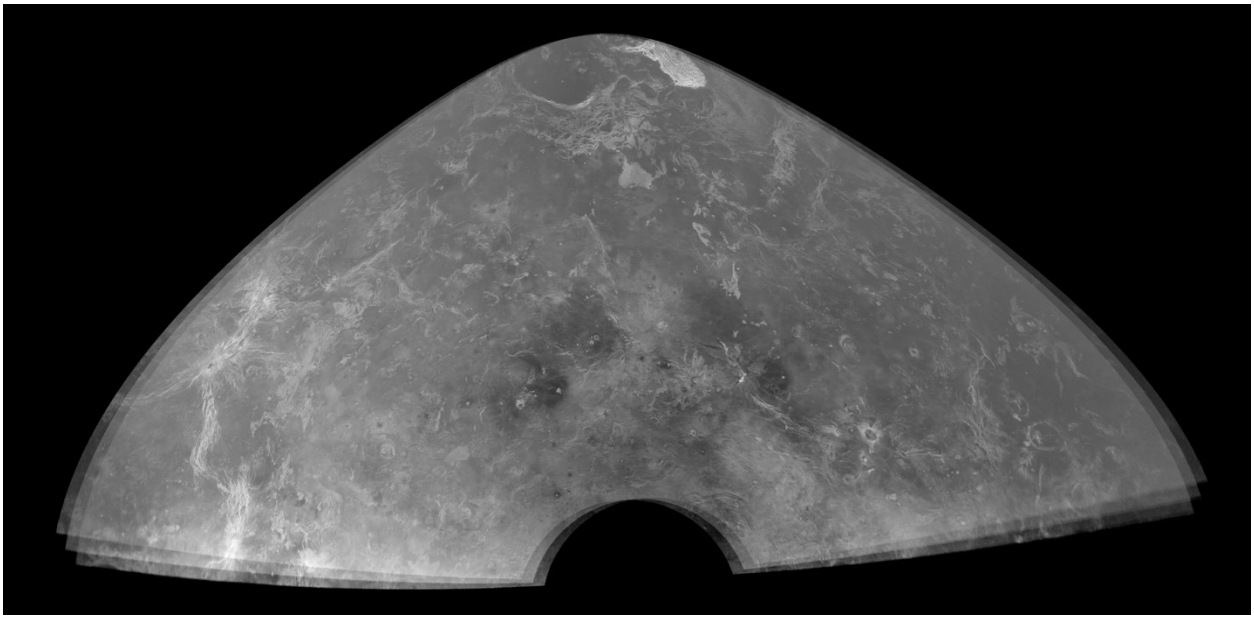

Fig. 5. OCP browse image map of the northern hemisphere from 2017, normalized to the scatter law from Fig. 4.

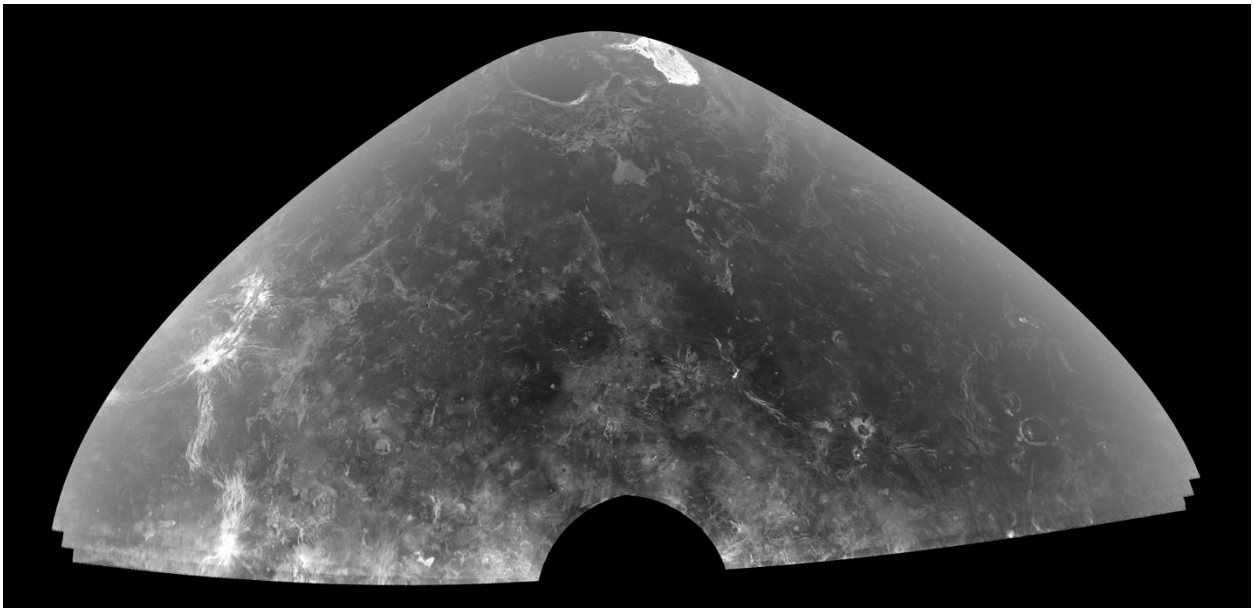

Fig. 6. SCP browse image map of the northern hemisphere from 2017, normalized to a cos(ϕ) scatter law.

Table 2. Sub-radar Point Locations and Number of Looks for Venus Observations

Year	Hemisphere	SRP_{LAT}	SRP_{LON}	Looks	Baud (μs)	Cal Factor (dB)
1988	N	1.36	334.24	28	4.0	+4.2
1988	S	-1.53	322.56	29	4.0	TBD
2012	N	-2.74	330.28	30	3.8	+2.6
2012	S	-2.68	330.62	TBD	3.8	TBD
2015	N	8.16	329.75	25	3.8	+1.6
2015	S	8.02	328.87	33	3.8	TBD
2017	N	-9.45	343.26	42	3.9	0.0
2017	S	-9.41	343.50	48	3.9	0.0
2020	N	-2.69	335.32	36	3.8	+4.7
2020	S	TBD	TBD	48	3.8	TBD

Tabulated SRP locations reflect averages over the 1-4 days of observations of a given hemisphere in each year, and may be used to calculate approximate incidence angles for each map pixel. Sub-radar point longitudes are corrected for refined spin rate from Campbell et al. [2019]. The baud is the time sampling of the round-trip echoes, yielding a one-way range resolution of ~600 m. Calibration factors are to be applied to the maps in each year to provide a relative calibration to the 2017 data.

References

Campbell, B.A., Campbell, D.B., and C. DeVries, Surface processes in the Venus highlands: Results from analysis of Magellan and Arecibo data, *J. Geophys. Res*., *104*, 1897-1916, 1999.

Campbell, B.A., Earth-Based Radar Observations of Venus, ARCB/NRAO-V-RTLS/GBT-3-DELAYDOPPLER-V1.0, NASA Planetary Data System, 2016.

Campbell, B.A., Campbell, D.B., Carter, L.M., Chandler, J.F., Giorgini, J.D., Margot, J-L., Morgan, G.A., Nolan, M.C., Perillat, P.J., and Whitten, J.L., The mean rotation rate of Venus from 29 years of Earth-based radar observations, *Icarus* 332:19–23. https://doi.org/10.1016/j.icarus.2019.06.019, 2019.